

Electronic Supplementary Material for Energy & Environmental Science.

This journal is © The Royal Society of Chemistry 2020

## **Supplemental Information**

### **Extra Lithium-Ion Storage Capacity Enabled by Liquid-Phase**

### **Exfoliated Indium Selenide Nanosheets Conductive Network**

Chuanfang (John) Zhang,<sup>1,\*</sup> Meiyang Liang,<sup>2,3</sup> Sang-Hoon Park,<sup>2,3</sup> Zifeng Lin,<sup>5</sup> Andrés Seral-Ascaso,<sup>2,3</sup> Longlu Wang,<sup>6</sup> Amir Pakdel,<sup>2,3</sup> Cormac Ó Coileáin,<sup>2,3</sup> John Boland,<sup>2,4</sup> Oskar Ronan,<sup>2,3</sup> Niall McEvoy,<sup>2,3</sup> Bingan Lu,<sup>6</sup> Yonggang Wang,<sup>7</sup> Yongyao Xia,<sup>7</sup> Jonathan N. Coleman<sup>2,4,\*</sup> and Valeria Nicolosi<sup>2,3,\*</sup>

#### **Affiliations:**

1 Swiss Federal Laboratories for Materials Science and Technology (Empa), ETH Domain, Überlandstrasse 129, CH-8600, Dübendorf, Switzerland

2 CRANN and AMBER research centers, Trinity College Dublin, Dublin 2, Ireland

3 School of Chemistry, Trinity College Dublin, Dublin 2, Ireland

4 School of Physics, Trinity College Dublin, Dublin 2, Ireland

5 College of Materials Science and Engineering, Sichuan University, Chengdu 610065, PR China

6 School of Physics and Electronics, Hunan University, Changsha 410082, PR China

7 Department of Chemistry, Shanghai Key Laboratory of Catalysis and Innovative Materials, Center of Chemistry for Energy Materials, Fudan University, Shanghai, 200433, China.

## **EXPERIMENTAL PROCEDURES**

### **Materials and Methods**

#### **(1) Synthesis of layered bulk InSe**

InSe was synthesized via a colloidal wet chemistry method. Typically, a mixture of 30 mL of hexadecylamine and 5 mL of dodecylamine was obtained and heated to 60 °C in a flask under a nitrogen atmosphere. Then, 1.69 mmol of indium acetate (InAcO) and 1.71 mmol of Se powder were added to the above mixture under stirring. The system was then heated to 150 °C and maintained for 30 min. After that, the reaction temperature was increased to 300 °C. After 4 h of reaction, the system was cooled down naturally to 60 °C, 10 mL of toluene was added to remove the residual amines. After centrifuging at 5000 rpm for 1 h, the supernatant was discarded and 35 mL of isopropanol (IPA) was added to the centrifuge tubes to redisperse the sediment, followed by another round of centrifugation at 5000 rpm for 10 min. After washing with IPA three times, the brown precipitates, which settled in the bottom of the centrifuge tubes, were collected and dried (under N<sub>2</sub> at room temperature) for further use.

#### **(2) Exfoliation of InSe NS and preparation of CNT dispersion**

InSe NS colloidal solutions were obtained through liquid-phase exfoliation (LPE) of the as-synthesized bulk InSe layered particles. First, a quantity of InSe powder was added to 20 mL of N-Methyl-2-pyrrolidone (NMP) to reach a concentration of 30 mg/mL. The suspension was bath-sonicated (P30 H Ultrasonic from Fischer scientific) for 6 h at an amplitude of 100% and frequency of 37 kHz, respectively. The sonication-generated heat was removed by a continuous flow of cooling water to ensure the bath temperature remained at ~20 °C. Once sonicated, the dispersion was subjected to centrifugation at 1000 rpm for 2 h. The top 60% of the supernatant was collected. To ensure a better processability, the exfoliated InSe was transferred from NMP to IPA. Through a high speed centrifugation at 10,000 rpm for 30 min, InSe exfoliated flakes settled in the bottom of centrifuge tubes. After decanting the supernatant, a small amount of IPA was added to redisperse the exfoliated InSe flakes to reach a concentration of 2.5 mg/mL. Single-walled carbon nanotubes (also P3-CNT, Carbon solutions Inc.) were dispersed in IPA at a concentration of 0.1 mg/mL using bath sonication. The sonication amplitude, time and frequency were set to 100%, 30 min, and 37 kHz, respectively.

#### **(3) Flexible InSe/CNT composite**

InSe/CNT electrodes were prepared using a vacuum filtration method. By blending exfoliated InSe suspensions and CNT dispersions and filtering through a polyethylene membrane (Celgard K2045, 0.06 μm pore size), several InSe/CNT flexible films were obtained with SWCNT contents being 5%, 10%, 20%, 30%. The mass loading and thickness of the electrodes were roughly similar. After filtration, the films (including

the membrane) were immediately transferred to a glove box (oxygen and water content < 1 ppm) to avoid potential degradation over time. The naturally dried films were then cut into individual electrodes with a diameter of 12 mm. The filter membrane was kept on the thin film electrode to serve as a secondary separator when used in coin cells. For the sake of comparison, bulk InSe, bulk InSe/CNT, exfoliated InSe films were also vacuum filtrated at similar thickness.

#### **(4) Li-ion coin cells assembly (half cells)**

We employed CR-2032 coin cells to evaluate the Li-ion storage behaviour of various electrodes. Typically, a layer of polypropylene membrane (K2045 coated PP, Celgard LLC, Charlotte, NC) was used as the separator. The thin film electrode (with attached PP) was used as the working electrode, while Li metal discs with a diameter of 16 mm were used as the counter and reference electrodes. 1 M lithium perchlorate ( $\text{LiClO}_4$ ) dissolved in ethylene carbonate (EC) and dimethyl carbonate (DMC) in a volume ratio 1:1 was used as electrolyte. Stainless steel discs were used as the current collector. For comparison, we also assembled coin cells based on bulk InSe, bulk InSe/CNT and exfoliated InSe films.

#### **Materials characterization**

The SEM images of all samples were acquired on a Zeiss Ultra Plus (Carl Zeiss, Germany) with an acceleration voltage of 2 keV. Energy-dispersive X-ray spectroscopy (EDX) was performed in the same microscope and analysed using the INCA program. The flake dimensions were statistically analysed based on SEM images by measuring the longest axis of the nanosheets and assigning it as the length. TEM images of all samples were performed on a FEI Titan at 300 kV (FEI, USA). Prior to the TEM study, the nanosheet dispersion was drop-casted onto holey carbon grids (Agar Scientific, UK). X-ray diffraction (XRD) and Raman spectroscopy were employed to examine the compositions of samples. The XRD patterns were obtained using a fully automated Bruker D5000 powder diffractometer equipped with a monochromatic  $\text{Cu K}\alpha$  radiation source ( $\alpha = 1.5406 \text{ \AA}$ ). The  $2\theta$  angles were set ranging from 20 to 40°, with a step size of 0.05°. Raman spectra of exfoliated InSe/CNT were acquired using a WITec Alpha 300 R with a 532-nm excitation laser at a power of  $\approx 150 \mu\text{W}$ . A 100× objective was used, with a spectral grating of 1800 lines  $\text{mm}^{-1}$ . The characteristic spectra for each sample were obtained by averaging 20 discrete point spectra. Raman mapping was obtained by acquiring  $80 \times 80$  spectra. Maps representing the presence of CNTs were generated by mapping the intensity of the CNT G band, whereas the presence of InSe was represented by the intensity of the InSe  $A_1'$  band. We painted two parallel contacts with silver paint (Agar Scientific) on the thin film electrode strips. The resistance of each sample was measured using a Keithley 2400 source meter unit. The electrode thickness was determined with a digital micrometer (Mitutoyo), based on which the electrical conductivity of the thin films was converted. X-ray photoelectron spectroscopy (XPS) was performed using monochromated  $\text{Al K}\alpha$  X-rays from an Omicron XM1000 MkII X-ray source with an EA125 energy analyzer, which yielded

a maximum energy resolution of  $\sim 0.65$  eV. All the binding energy scale was referenced to the aliphatic carbon 1s core-level at 284.8 eV.

### **In-situ XRD**

Operando X-ray diffraction experiments were conducted using a Swagelok-type cell equipped with a beryllium window (X-ray transparent) as current collector. A lithium foil was used as both the counter and reference electrodes and Whatman glass fiber (GFA) as the separator. The filtrated InSe/CNT thin film (attached with PP) was utilized as the working electrode. 1 M lithium hexafluorophosphate (LiPF<sub>6</sub>) dissolved in ethylene carbonate (EC) and dimethyl carbonate (DMC) in a 1:1 volume ratio was used as the electrolyte. The electrochemical tests were performed on a VMP (Biologic France) during galvanostatic charge-discharge measurements. At the same time X-ray diffraction (XRD) patterns were recorded using a Bruker D8 diffractometer ( $\lambda_{\text{CuK}\alpha} = 1.5418$  Å) equipped with a LynxEye detector. It should be noted that for the 1st discharge, the discharge currents were modified several times for selecting a proper rate current to ensure enough XRD patterns were collected for each cycle (otherwise it would consume too much time).

### **Density function theory calculations**

The DFT calculations of the In<sub>x</sub> (x=3,4,5,7) nanocluster models were carried out using the optB88-vdw exchange-correlation functional. The geometries for the different models used were optimized until the forces on each relaxed atom were lower than 0.025 eV Å<sup>-1</sup> and the electronic structure at each geometry optimization step was self-consistently converged with energy, density, and eigenvalue thresholds of 5E-4, 1E-4, and 5E-8 eV, respectively. The exchange-correlation interactions were treated by generalized gradient approximation (GGA) parameterized by Perdew, Burke, and Ernzerh of (PBE). A vacuum region of 15 Å was added to avoid the interactions between adjacent images. The Brillouin zone was sampled by Monkhorst-Pack method with 5 × 5 × 1 k-point grid.

### **Electrochemical characterization**

To evaluate the electrochemical responses of the as-obtained samples, all half cells were measured using cyclic voltammetry (CV) and galvanostatic charge-discharge (GCD) with a voltage range of 0.05-3 V on a potentiostat (VMP3, Biologic). In the CV measurements, the cells were cycled 0.2 mV/s for 10 times. In the GCD tests, cells were charged-discharged at various current densities ranging from 100 mA/g to 2000 mA/g. The capacities of the electrodes were obtained from the stabilized cycle (6th cycle) at each current density and normalized to the mass of active material (InSe). For the cycling tests, the cells were charged-discharged at 1000 mA/g for 100 cycles or at 500 mA/g for 260 cycles. After relaxing for 2 weeks, the cell was charge-discharged again at 500 mA/g for another 640 cycles.

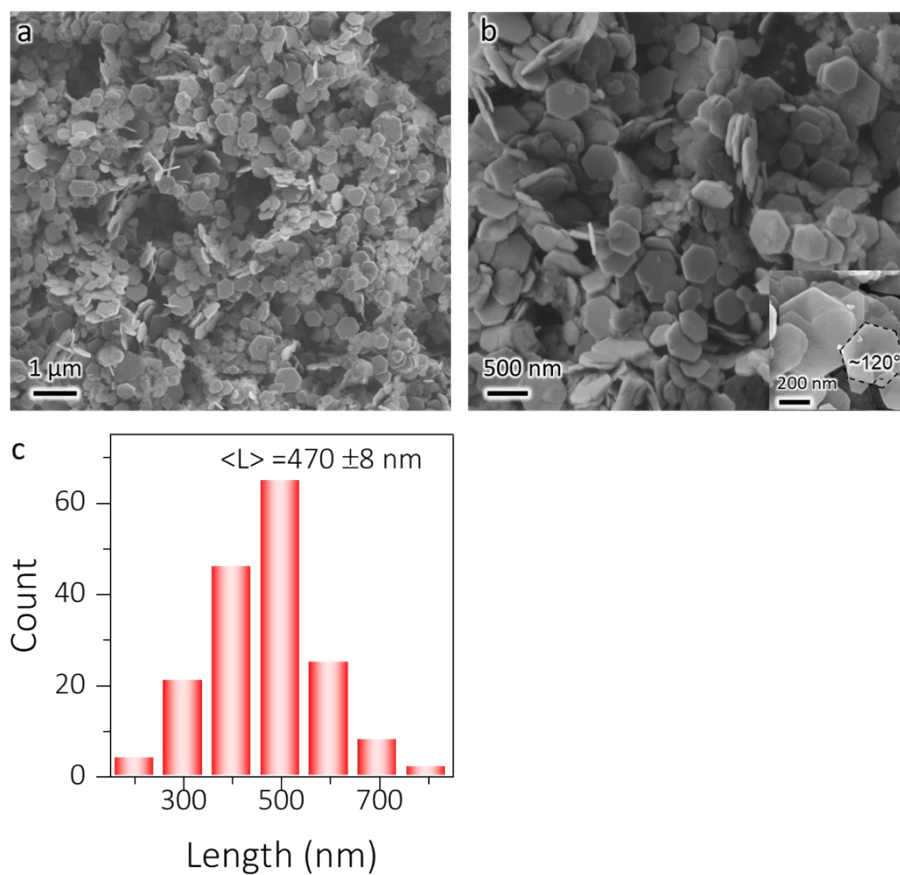


Figure S1. (a-b) SEM images of as-synthesized layered InSe crystals under different magnifications, showing a uniform hexagonal morphology. Inset in (b) is a typical hexagonal crystal with edge angle  $\approx 120^\circ$ . (c) The size distribution of as-synthesized layered InSe, showing an average lateral size of  $470 \pm 8 \text{ nm}$ .

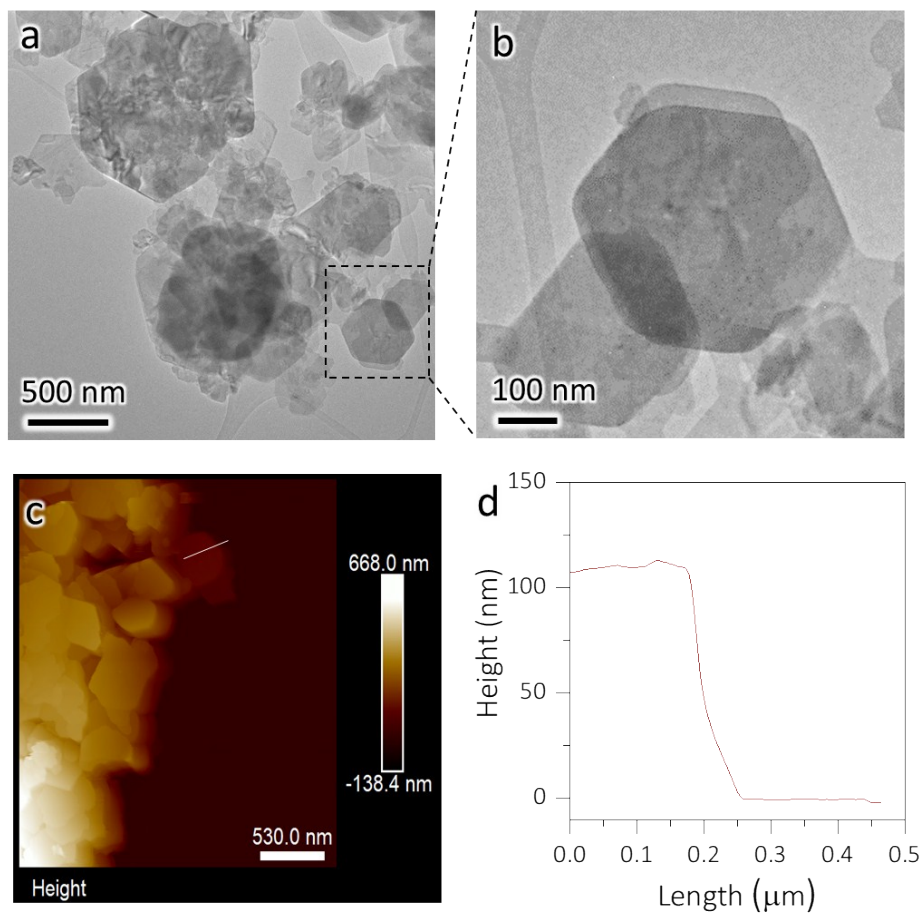


Figure S2. (a) Typical TEM image of as-synthesized layered InSe crystal. (b) Enlarged TEM image of the dotted area in (a), showing a hexagonal shape of the layered InSe. (c) AFM image of the as-synthesized layered InSe. We note that the platelets tend to aggregate during the AFM sample preparation, rendering it quite challenging to obtain the intrinsic thickness of the flake. Despite that, we still managed to find one flake that dispersed separately, and obtained its height profile along the line in (c), as shown in (d).

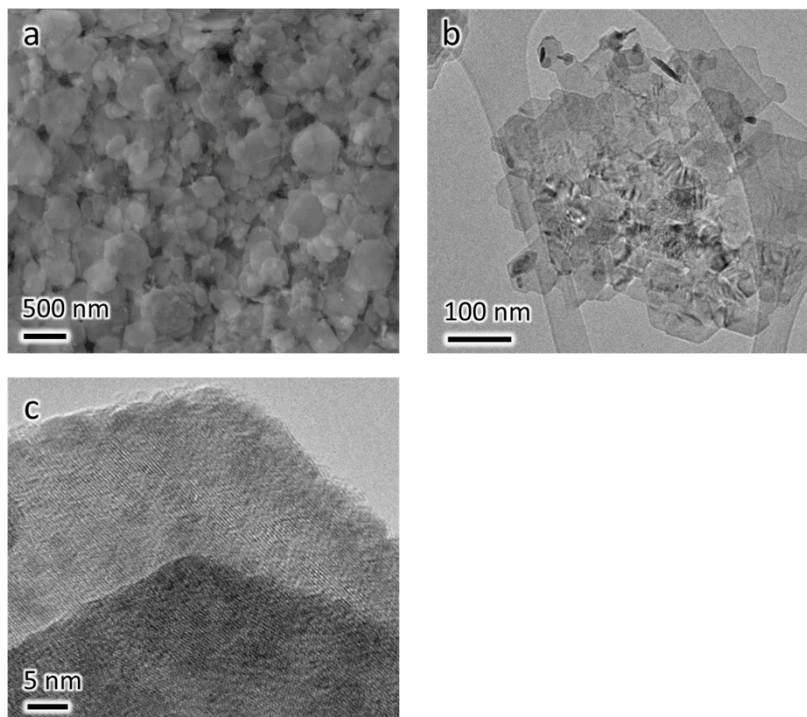


Figure S3. (a) SEM, (b) TEM and (c) HRTEM images of the exfoliated FL-InSe flakes. The flakes are highly crystalline and ultrathin, as they are electron transparent in (b).

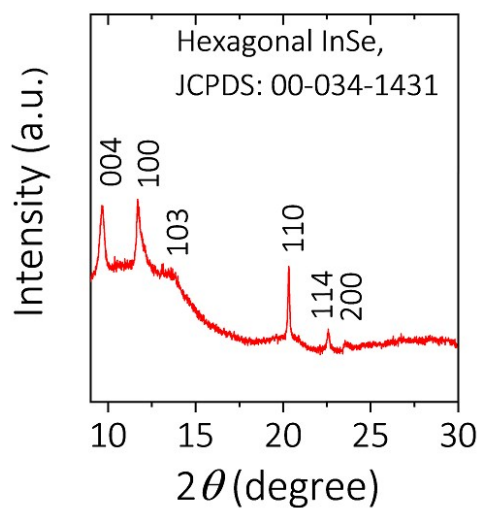


Figure S4. XRD pattern of exfoliated FL-InSe flakes, showing an identical structure to that of layered bulk InSe.

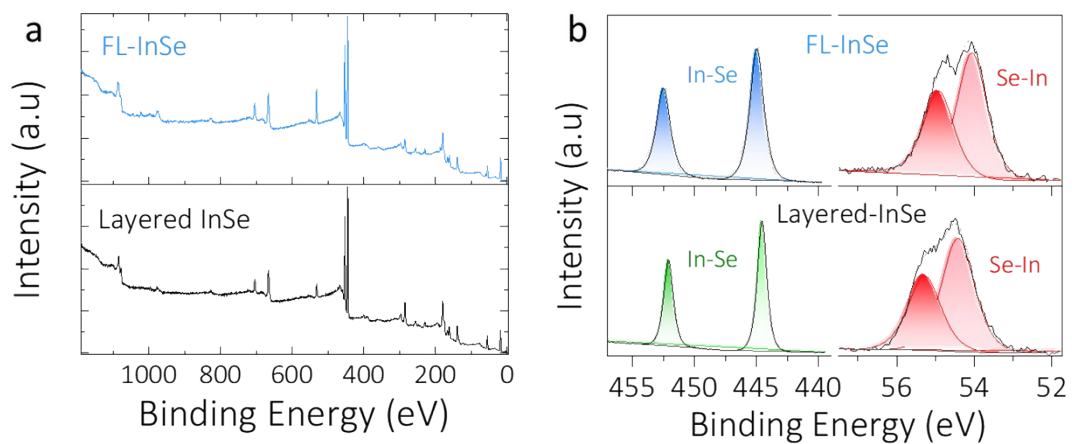


Figure S5. XPS spectra of layered InSe and FL-InSe with (a) survey and (b) In and Se core-level spectra. The almost identical spectra before and after LPE process suggest the exfoliation did not introduce apparent degradation of InSe.

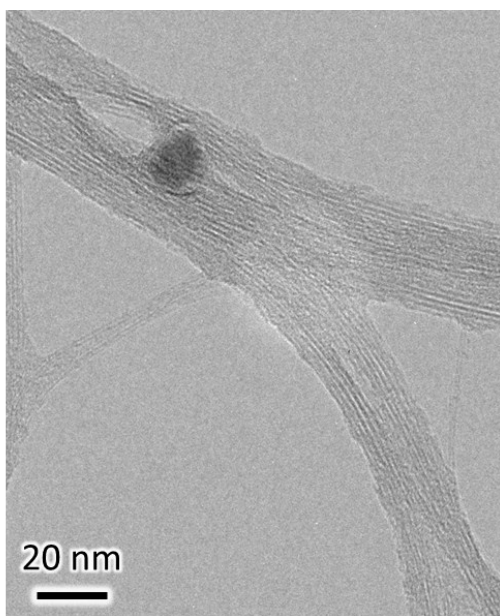
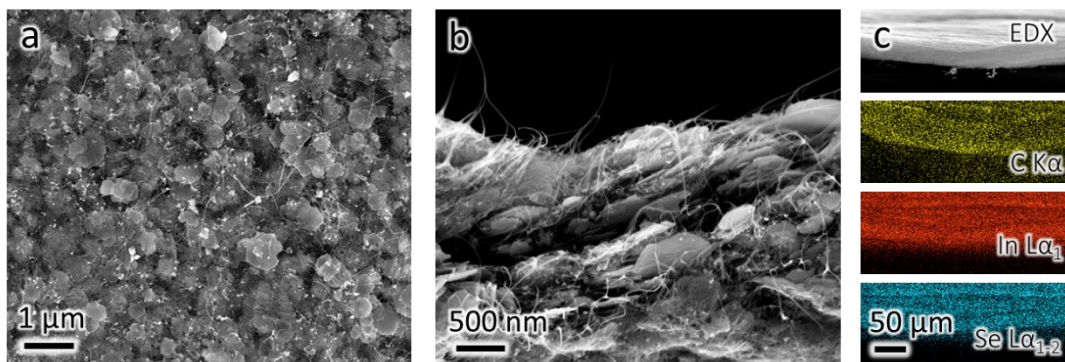
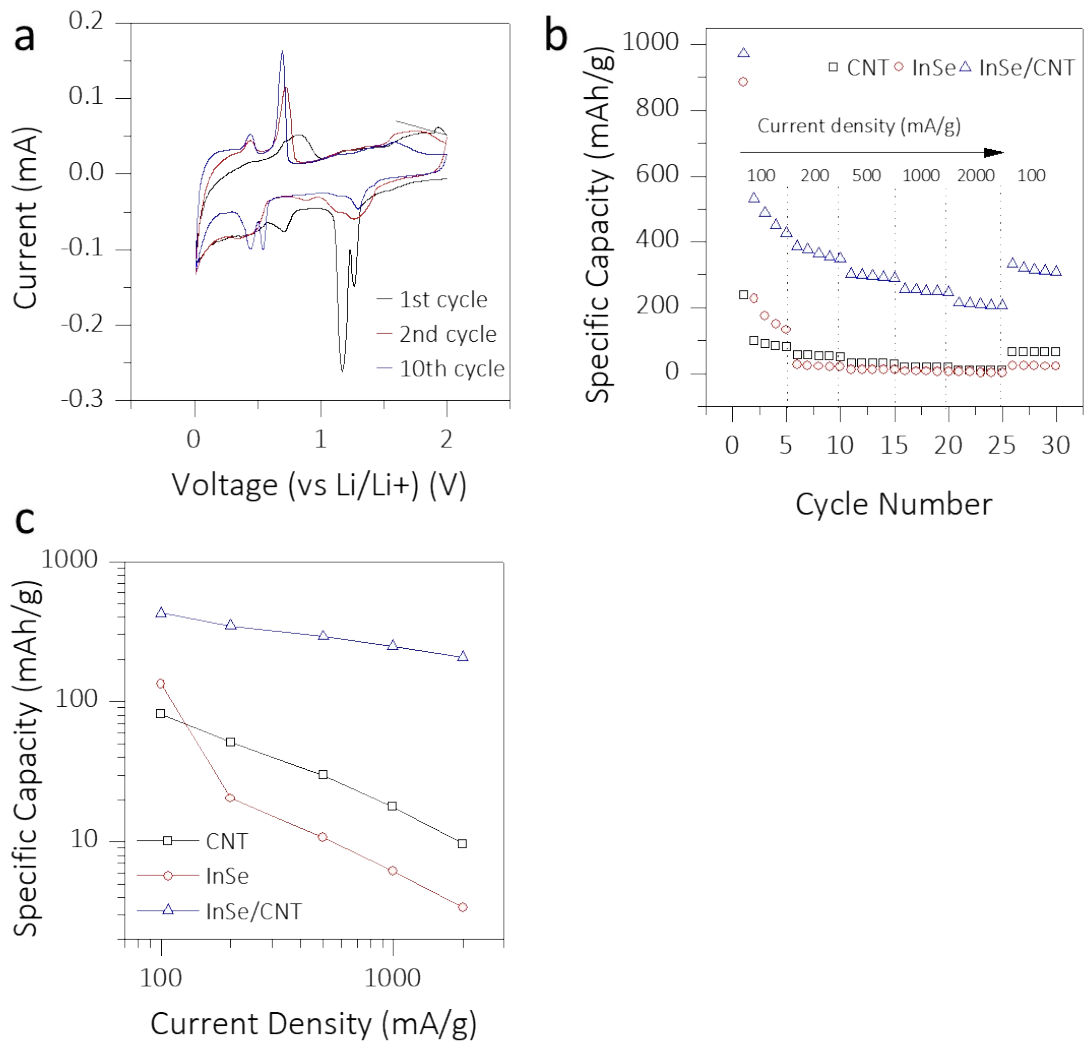


Figure S6. TEM image of CNTs, showing bundles and defects on the nanotube walls.



**Figure S7.** (a) Top view and (b) cross sectional SEM images of FL-InSe/CNT electrode, showing a homogeneous distribution of the exfoliated InSe flakes. This is further confirmed through the EDX mapping of C, In and Se in (c).



**Figure S8.** (a) CV curves of layered InSe/CNT at 2 mV/s. (b-c) Rate performance of CNT, bulk InSe, and layered InSe/CNT electrodes at different current densities.

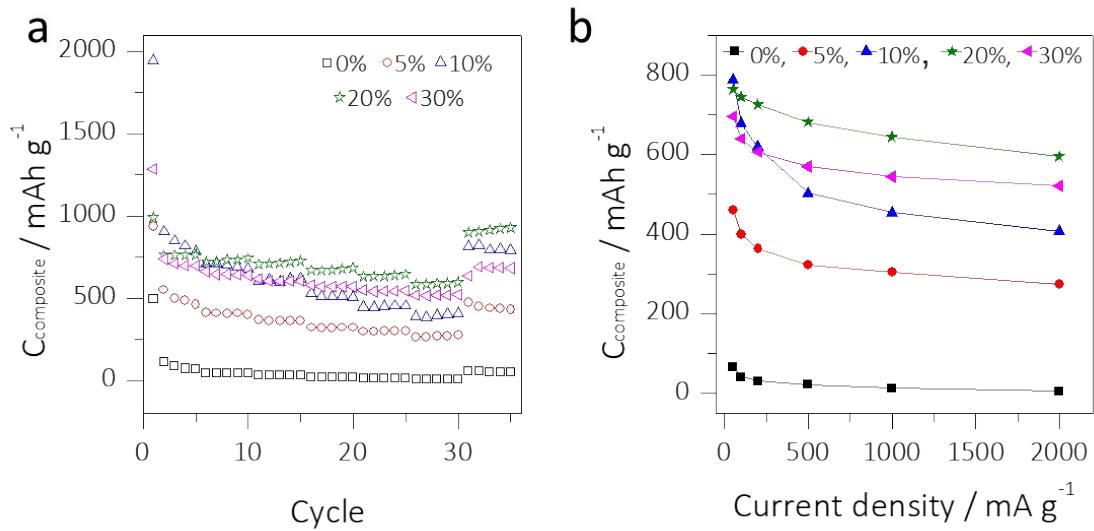


**Figure S9.** Rate performances of different FL-InSe NS/CNT composites as a function of (a) cycling and (b) current density.

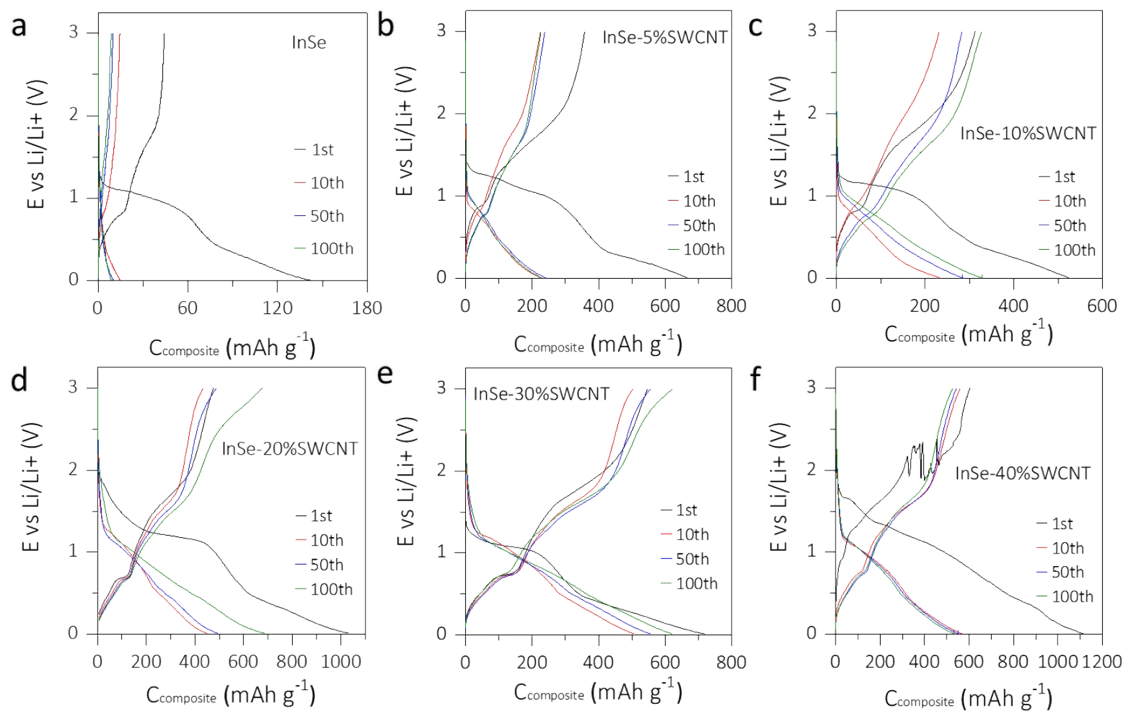


**Figure S10.** GCD profiles of various electrodes with different CNT contents under different cycles.

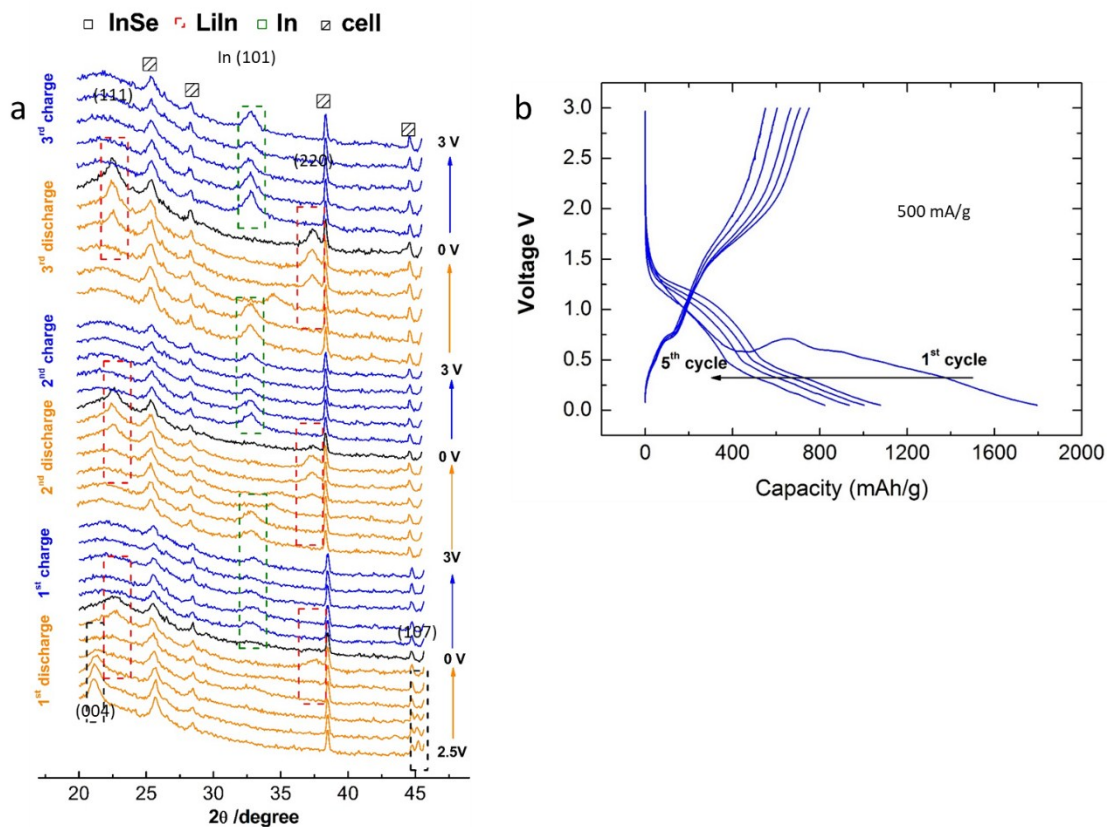


**Figure S11.** (a) In-situ XRD patterns and (b) GCD profiles of FL-InSe/CNT under different cycles.

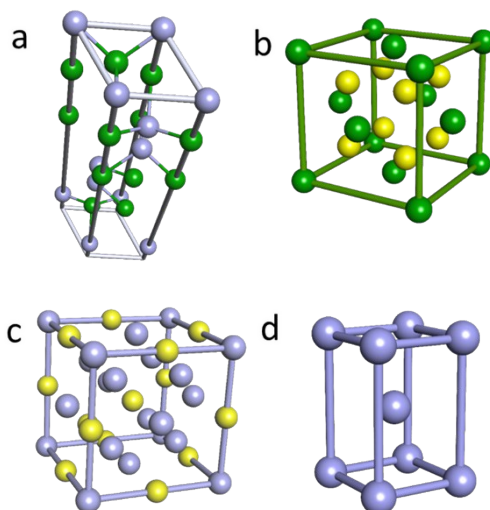


**Figure S12.** Atomic structures of an unit cell of (a) InSe, P 63/mmc (#194-1), (b) Li<sub>2</sub>Se, - F m -3 m (#225-1), (c) InLi - F d-3m (#227-1) and (d) In - I 4/mmm (#139-1).

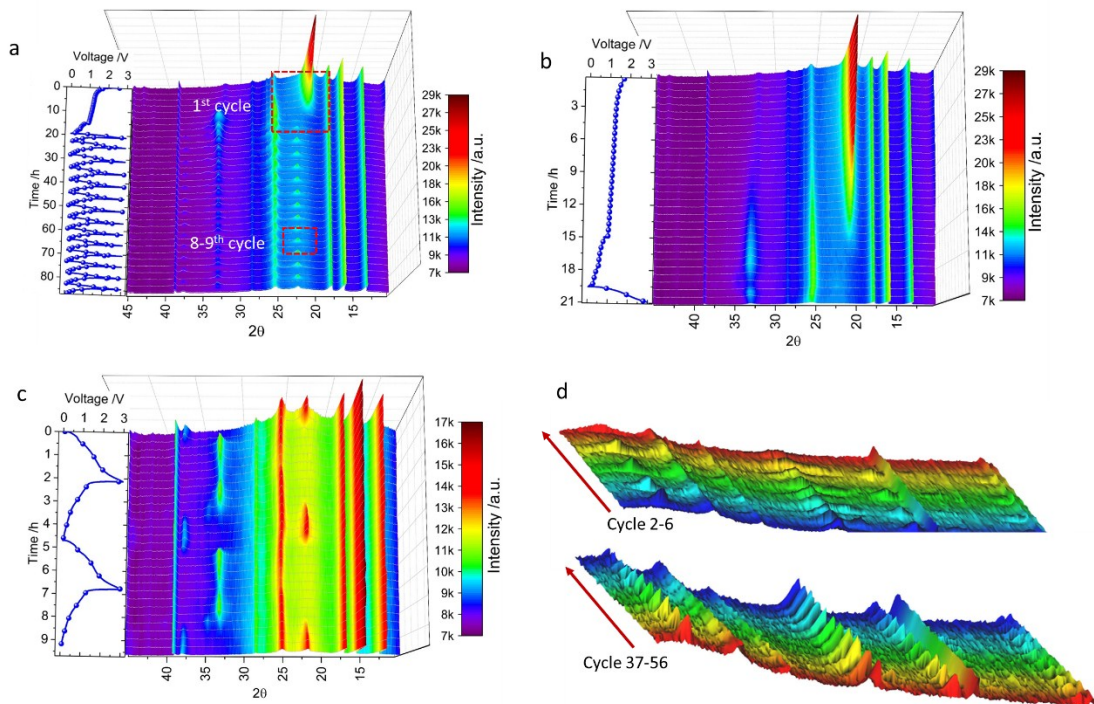


**Figure S13.** Operando XRD measurement patterns of FL-InSe/CNT electrode demonstrated in three-dimensional manner at (a) cycle 1 to 14, (b) cycle 1, (c) cycle 8,9 and (d) cycle 2-6 (up panel) and cycle 37-56 (bottom panel).

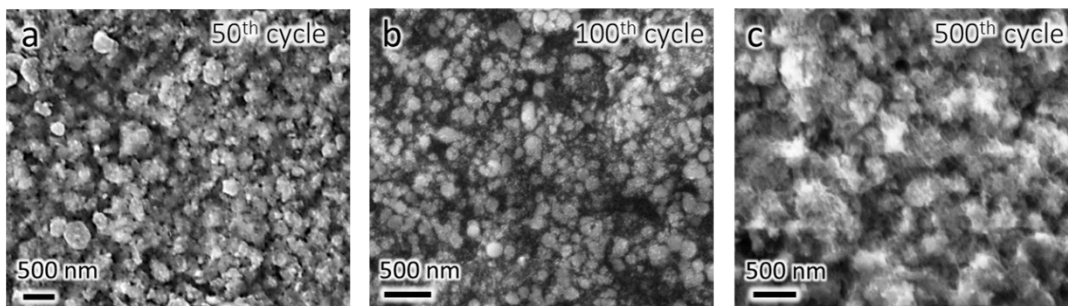


**Figure S14.** Post-cycling SEM images of the FL-InSe/CNT electrode after (a) 50 cycles, (b) 100 cycles and (c) 500 cycles. Clear nanoclusters are observed in (c), verifying the DFT calculation results that In clusters formed upon repeated cycles.

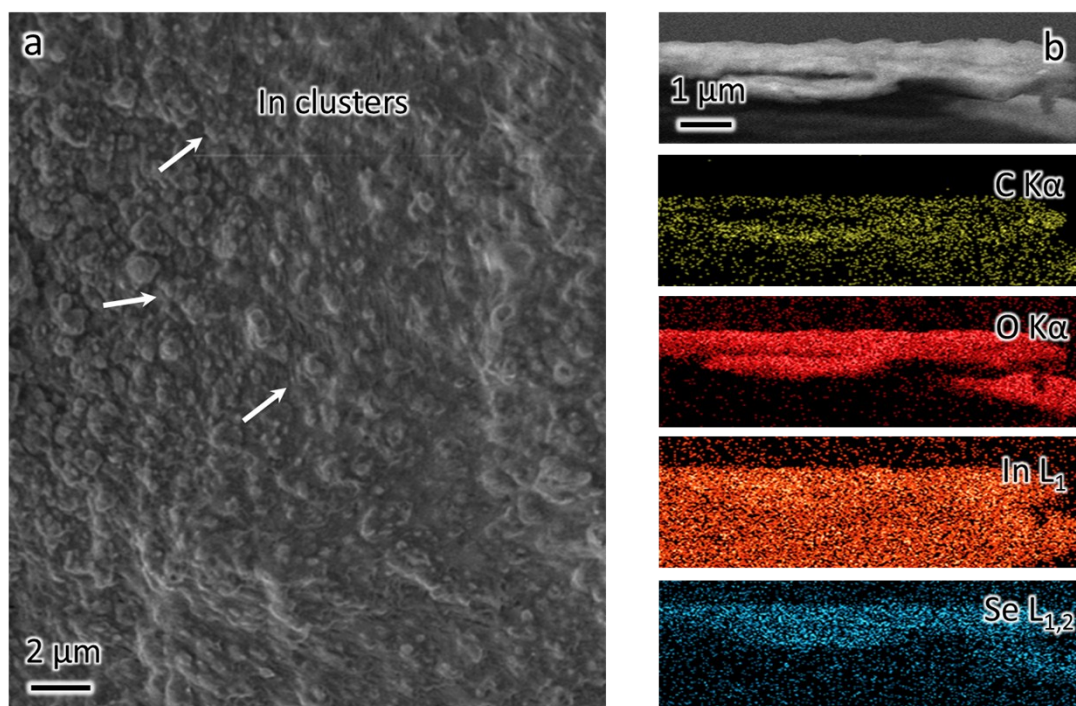


**Figure S15.** Post-cycling SEM image of the FL-InSe/CNT electrode after 500 cycles and stopped after charging to 3 V (a), showing abundant In clusters. The EDX mapping of this cycled electrode can be found in (b), showing a random distribution of In clusters that differ from the sharp C and O edges. The blurred edges in the Se signal particularly does not overlap with In signal, implying that Se no long bond to In; instead, it lithiates/delithiates with Li.